Digital System for Detecting, Classifying, and Fast Retrieving Corrosion Generated Defects

S.T. Kyvelidis, L. Lykouropoulos, and N. Kouloumbi—National Technical University of Athens*

The in-situ assessment of the degradation of a coating system is often difficult, especially in cases such as underwater piping systems. Furthermore, the results of the optical inspection are qualitative and subjective. The use of digital image processing and storing of corrosion images in databases can eliminate such problems and enhance the assessment of the coating degradation characteristics.

Digital defect detection systems have been used in the industrial domain for the last 20 years to automatically detect and classify defects on various surfaces, such as wood, steel, and textiles, using image processing techniques and decision-making theory.

The proposed system processes digitized images of corroded surfaces by applying similar technologies (digital filters, texture analysis, segmentation techniques, and fuzzy decision algorithms) to automatically identify and classify corrosion generated defects, such as blisters, rust, etc. Furthermore, it employs state-of-the-art database techniques specialized for image content (query by example, content-based retrieval) to effectively store and retrieve these images according to their specific features.

INTRODUCTION

Optical observation, combined with results obtained from electrochemical methods, has often been used in the evaluation of corroded systems.[1] The commonly followed practice is based on the optical comparison of the system under study with standard corrosion images. This approach, although simple and straightforward, has certain disadvantages. For example, the optical inspection varies from person to person as each inspector judges a system subjectively. Also, certain types of failure are difficult to identify, especially in cases where the in-situ inspection is difficult, as in the case of underwater constructions.

Digital image acquisition, processing, and interpretation techniques have been successfully employed in the industrial domain for the last 20 years to automatically detect and classify defects on various surfaces, such as wood, steel, and textiles.[2] Similar techniques have been employed in the past for the evaluation of corrosion generated defects.[3-9] This approach offers certain advantages such as (a) finding information hidden from the human eye, (b) quantifying the defect features that can be used for comparison with similar data from other images and with data from electrochemical methods, and (c) building a database with corrosion images.

The proposed system uses standard image processing techniques in order to identify possible corrosion-generated defect areas. Furthermore, it uses smart algorithms that attempt to automatically classify these areas in certain defect categories, which are predefined by the inspector. Finally, it uses advanced database techniques by employing some of the latest developments in the field of database research technology. This gives the inspector the opportunity to perform complex query operations on the image data and to connect the images to their specific data and to the data obtained by other types of measurements.

*Chemical Engineering Dept., Materials Science and Engineering Section, Iroon Polytechnioy 9, Athens, Greece, Tel. 30-1-772-3101.

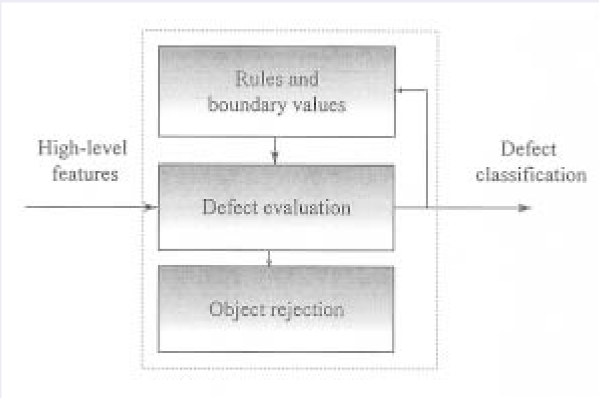

Figure 1—Defect classification block diagram.

DESCRIPTION OF THE SYSTEM

The system operates in two stages. The first is the image processing stage followed by an image storage and retrieval process.

Image Processing

The processing of a digital image consists of a number of steps that aim to extract specific information from it. The first step is the acquisition of the digital image using a photographic camera or a video camera and the digitization using a digitizing device (scanner or the camera itself). The second step is the preprocessing of the image, where preprocessing algorithms are applied and finally a segmentation process follows.

The preprocessing deals with the enhancement of the original image in order to eliminate noisy information and to increase image contrast. Depending on the type of image, different image enhancement techniques can be applied. Generally, low- and high-pass filters are used pair-wise. The low-pass filter reduces speckles (isolated pixels) and the high-pass filter eliminates the blurring effect caused by the low-pass filter. For low-contrast images, histogram stretching, and direct histogram specification techniques are afterwards applied.[10]

Segmentation is the procedure that separates and detects regions (objects) of the image that may be labelled at later stages of processing as defect areas. The type of segmentation algorithm that is used depends on the characteristics of the image.[11] For uniform surfaces a threshold-based technique is applied. More specifically, a gray-level value l is automatically found using local histograms of gray-level values. For color images the value l is calculated as $l=(r+g+b)/3$[10], where r,g,b are the intensities of the red, green, and blue components of color. The value l is then used as a threshold value to separate the regions. This method is not always precise, since threshold-based techniques require a Gaussian distribution of defect gray-level values around a mean value to make discrimination possible between defective and non-defective regions, which is not the case for all types of our images.

To enhance region-based segmentation in those cases, watershed-based segmentation[12] is used as a reliable means of locating local minima and maxima in the image where defects are treated as local 'basins.' By combining threshold-based techniques and watershed segmentation, the resulting image is a black-and-white image where black indicates possible defects and white corresponds to non-corroded areas.

After the region boundaries have been almost clearly set, low-level features (features independent of image objects) are extracted that correspond to shape, position, color, and texture of regions (objects).[13] For shape and position, the minimum bounding rectangle (MBR) (that includes the object without intersecting it), the moments of the object (major and minor axis, x and y centroids and area in pixels), and the polygonal approximation of the object are stored after an edge detection algorithm is applied (i.e., an array of vectors that describes the object boundaries). For texture, a set of statistical texture measures[9,14] (an array of values that describes the texture of the object) is calculated. Texture is a feature of the image which is independent of color and is connected to the spatial arrangement of pixel inside an area. Finally, for the color representation, the color distribution (a cumulated histogram of colors[15] within the object) is found.

Using the low-level features, the system calculates high-level features for each object (features that are important to defect analysis and can be used for queries, as explained later). These are the object areas in some area measurement units, the dominant color of a defect, the dominant orientation of the defect within the image, the shape (roundness, fractal dimension of the boundaries), and the absolute position of a defect inside the image. Also, according to the statistical measures calculated, the texture is assigned one textual attribute (fine, coarse, smooth, etc.) using the visually important measures of texture.[14]

After the high-level features have been found for every object of the image, certain rules are applied that aim at defining the defect type of the object.[16] The objects are categorized to specific predefined types of defects called defect «classes». Objects that do not belong to any predefined class of the system after the application of the rules are labeled as «Unknown». These objects can be used later for algorithm enhancement and modification. The characteristic features that define the type of defect are its shape, size, color, and texture. Shape roundness, for example, can be very useful when looking for blisters and color can be very indicative of rust existence.

Table 1—Image Table

Field	Type
Image_id	Number, id of image (system given)
Filename	Text, system filename of the image
Date	Date, the date taken
System_Data	Date, the date stored (automatically filled)
Origin	Text, source of image
Description	Text, a free description of the image
P-to-m	Number, a ratio used to convert pixels to mm.

The rules used are based on fuzzy operations along with empirically given boundary values. The defect classification system takes as input the values of the features for each object along with the values for the given class of defect and evaluates the defect type (*Figure* 1). If the system fails to detect an object or gives a non-satisfactory answer, the inspector can manually alter the boundary values or the rules themselves and repeat the process. An example of a blister detection rule could be the following (expressed in an English-like language):

Table 2—Defect Table

Field	Type
Defect_id	Id of the defect
Image_id	Number, id of the source image
Description	Text, a free description of the defect
DefectType	Text, a defect class
MBR	4 Numbers, two (x,y) coordinates of the MBR
CenX, CenY	2 Numbers, centroid x and y
Major axis	Number, major axis length
Minor axis	Number, minor axis length
Shape_Roundness	Number, the ratio of major to minor axis
Fractal dimension	Number, a measure of the shape irregularity
R, G, B of dominant color	Numbers between 0 and 255 showing dominant color
Texture	Text, the texture type
Area	Number in pixels
Orientation	Number in grads
ParentDefect_id	Number, NULL, in case of macroscopic defect or parent id

if shape_roundness is > 0.8
  and texture is not fine
  and area is < 1.5
  and color is between dark_green and light_green
then
  defect_class = (blister, 90%)

This means: if the defect found is round, its texture is not fine, the area of the defect is lower than 1.5 mm^2, and its color is darker or lighter than the surface color (green), then this defect is with 90% certainty a blister.

It is possible that an object cannot be classified to a certain defect type. For example, small dots in the image can either be the result of rust or pitting formation or even a rule failure. In that case, these objects are classified with a level of uncertainty to more than one defect type.

For example:

if area < 0.5
  and shape_roundness is > 0.9
  and color is like black
then
  defect_class = (pitting_component, 40%)
or
  defect_class = (rust_component, 40%)

which means that if the object is very small (area < 0.5 mm^2), round-shaped, and black then it must be rust, the result of pitting formation or a failure of the rule.

In this case, the macroscopic defect is found by applying rules for multiple objects. The system finds if the objects are localized (if they form a cluster) or if they are randomly distributed. For every cluster it applies rules and classifies them to a macroscopic defect type. If the rules do not apply, the objects are not classified to a specific defect (e.g., random noise or isolated marks).

Image Storage and Retrieval

The images and their classified and unclassified objects are stored in a database. The database is designed in such a way that it (a) permits the user to quickly search and retrieve defect-specific data and (b) can support complex query operations. The database schema supports textual, numeric, and spatial data (data that describe position and shape of objects). Furthermore, it supports data obtained from electrochemical measurements, such as the electrochemical impedance spectroscopy (EIS), which are inserted via spreadsheets. The structure of the database varies according to the type of measurements included. It can be easily extended to hold any type of measurement in its structure.

To be able to answer spatial queries quickly («show images of rust spots within a range of 5 mm^2») and also display an object upon request, the system stores the defect MBRs in the database. Using the benefits of recent research on spatial database technology,[17-18] specialized data structures called R-trees are used, which can efficiently store and retrieve spatial arrangement information of objects using their MBRs. The database structure is the following: First, each image with its relevant data (date, origin, description, etc.) is stored in a table format (see *Table* 1).

For every image, the data of defects is also stored. Since some defects form a wider (macroscopic) defect (e.g., in the case of blistering, the total area of all the small blisters) the database is designed so that it can store the hierarchical relationship of such objects. To simplify design and to still be able to retrieve this relationship, the microscopic and macroscopic defects are both stored in the same table («self-join» implementation of relational databases[19]). The field «ParentDefect_id» of *Table* 2 serves this implementation.

The electrochemical data are stored in a separate structure (*Table* 3a). The impedance table contains the header information of the measurement. The data itself is stored in a separate table (*Table* 3b) for design efficiency.

The schema can be easily stored within any relational database (like Access, dBase, Oracle, etc.) along with their indices to data. MBRs are also stored in an external index file to serve range queries (*Figure* 2).

The retrieval of information is achieved using a structured query language (SQL)-like syntax.[20] The queries can contain table fields, spatial operators (range), and values. The composed query is passed to a query proces-

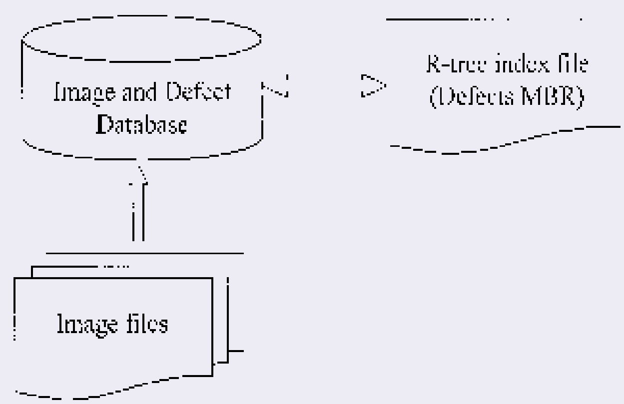

Figure 2—Image database schema.

Table 3—Impedance (a) and Impedance Data Table (b)

a. Impedance

Field	Type
Meas_id	Number, measurement id
Image_id	Number, id of image
Date	Date, date of measurement
Description	Text, free description

b. Impedance_data

Field	Type
Meas_id	Number, measurement id
f	Number, frequency
Z	Number, impedance
Φ	Number, phase angle

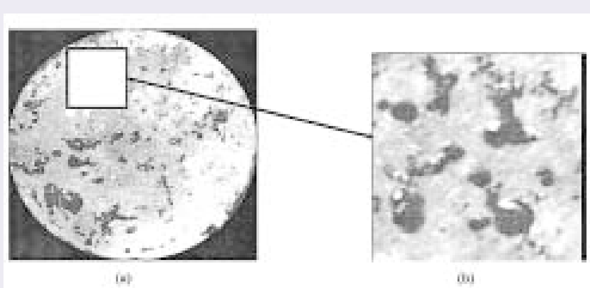

Figure 3—Sample image of a corroded steel specimen coated with an epoxy resin coating. (b) Detail of the image of the previous image.

sor that in turn queries the database and, if necessary, the R-tree index file. An example query in SQL-like syntax that returns all the images containing rust defects with area between 2 and 5 mm^2 is the following:

Select distinct Image_id from Defect, Image where Image.Image_id=Defect.Image_id and Defect.Defect Type = 'rust' and Defect.Area > 2 and Defect.Area <5.

A more complex query can also be formulated such as «find the images with rust defects with average area between 2 and 5 mm^2». Furthermore, using the query-by-pictorial-example (QPBE) technology of Image DB and a visual interface, the system can find images with similar defect types using an example image.[21-24]

APPLICATION OF IMAGE ANALYSIS SYSTEM ON SPECIMENS COATED WITH IRON POWDER FILLED EPOXY RESINS

Using the system described previously, the anticorrosive performance of epoxy resin coatings filled with iron powder was investigated. The test specimens consisted of steel disks of 6 cm diameter coated with epoxy resin which was filled with 15 and 30% w/w iron powder. Specimens coated only with epoxy resin were also prepared as reference specimens. The composition of the steel substrate (in % wt) was 0.12 C, 0.5 Mn, 0.005 S, and the balance was Fe. The epoxy was a bisphenol A-based epoxy resin of about 1025 molecular weight with an epoxy equivalent weight 500-535, viscosity 30-40 sec (DIN 53211, 4 mm, 20°C), and density 1.00-1.02 gr/cm^3 at 20°C. A high viscosity polyaminoamide with amine value (DIN 16945) 240-260 was used as a curing agent. The ratio resin/curing agent was 200/65, according to the manufacturer's data sheet. The iron powder used (Ferak Lab.) consisted of spheroid particles with an average particle diameter of 52 μm. The preparation of specimens is described in detail in earlier publications.[25,26] The coatings were immersed in a corrosive environment of 3.5% w/w NaCl for a time period up to 300 days. EIS measurements were also performed.

Figure 3 presents a photo of a steel specimen coated with a pure epoxy resin coating immersed in a corrosive environment for 230 days. The sequence of *Figure* 4 shows the various processing stages of the analysis of a detail of the image of *Figure* 3.

Initially a smoothing filter (low-pass) and a sharpening filter (high-pass) were applied to the original image (*Figures* 4a and b) in order to eliminate noise from the image digitization and enhance image contrast. The resulting image was convenient for edge detection. Then the picture was segmented (*Figure* 4c) using a thresholding algorithm. At this stage some noise still existed (isolated black pixels). This noise was removed using a despeckling algorithm (*Figure* 4d). Finally, the object boundaries are found and the objects are numbered (*Figure* 4e). After the objects have been detected and classified, certain features are calculated, which in this case were the spot area and the spot axis ratio.

This procedure was followed for the iron-filled epoxy resin coatings as well. The frequency distribution of the

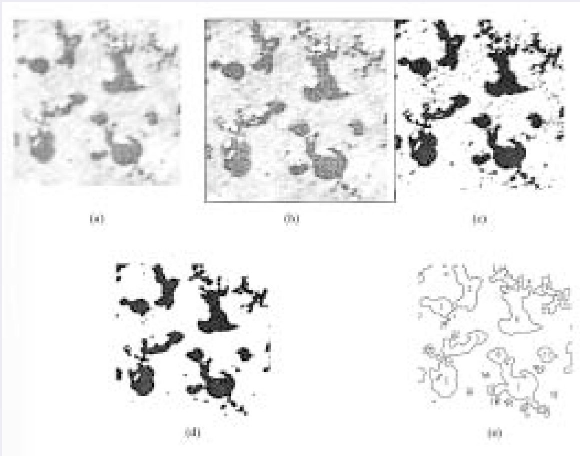

Figure 4—Image Processing of photo of a corroded steel specimen coated with an epoxy resin coating.

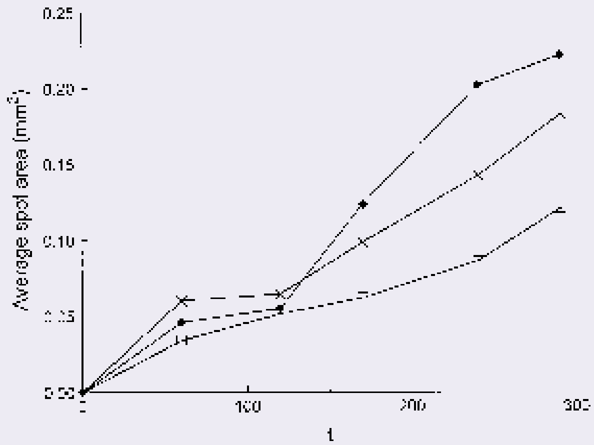

Figure 6—Average spot area vs. exposure time at 3.5% NaCl.(□) Pure epoxy resin coatings, (x) epoxy resin coatings filled with 15% w/w iron powder, (♦) epoxy resin coatings filled with 30% w/w iron powder.

corrosion spot area for the pure and the iron-filled epoxy coatings after 290 days of immersion is shown in *Figure* 5. The histogram reveals a wider spread of corrosion spot sizes (with size < 6 mm^2) for the 30% iron-filled coatings compared to the 15% iron-filled coatings and the pure epoxy coatings.

By performing this analysis at various immersion times and calculating average values for the corrosion spot areas, one can estimate the growth of the corrosion spots throughout the immersion period. Such a plot is presented in *Figure* 6. A two-step progress is evident for all types of coatings. Initially the values of the average spot areas increase with time, and at about 120 days of immersion they tend to stabilize at a certain value. After 150 days the values increase almost linearly up to 300 days of immersion, while the rate of growth for the iron-filled coatings is bigger compared to that of the pure epoxy coatings.

Figure 7 presents the average number of corrosion spots found in the exposed area of the samples (≈ 16 cm^2). The figure indicates that after 290 days of immersion, the pure and the 15% iron-filled epoxy coatings exhibit almost the same number of corrosion spots, while fewer spots are found for the 30% iron-filled epoxy coatings. This conclusion is in agreement with earlier observations that the iron powder loading protects the coating by a barrier mechanism and slows down the process of the corrosion spot creation.[25,26] On the other hand, the

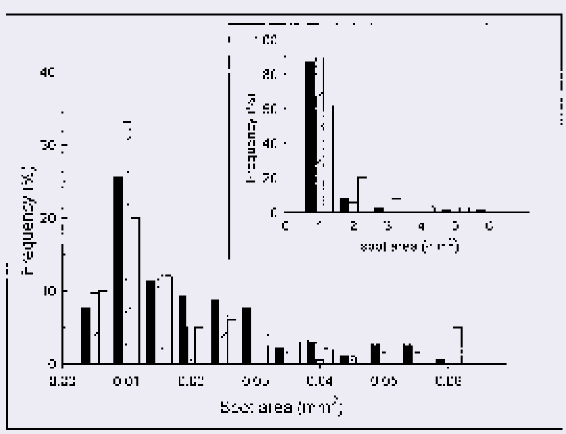

Figure 5—Frequency distribution of the corrosion spot area. The inset histogram shows a wider scale of areas. The black bars represent pure epoxy resin coatings. The dashed bars represent epoxy coatings filled with 15% w/w iron powder and the hollow bars represent coatings filled with 30% w/w iron powder.

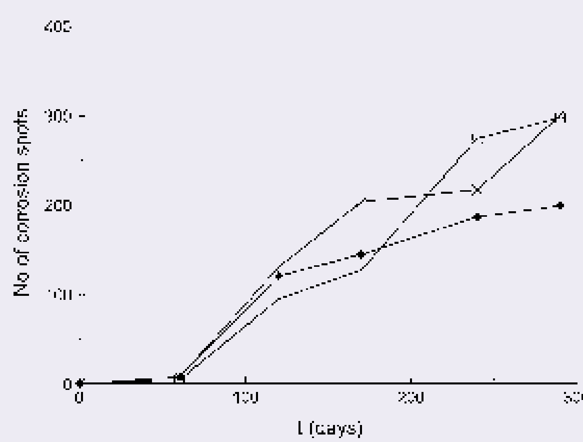

Figure 7—Number of corrosion spots vs. exposure time at 3.5% NaCl.(□) Pure epoxy resin coatings, (x) epoxy resin coatings filled with 15% w/w iron powder, (♦) epoxy resin coatings filled with 30% w/w iron powder.

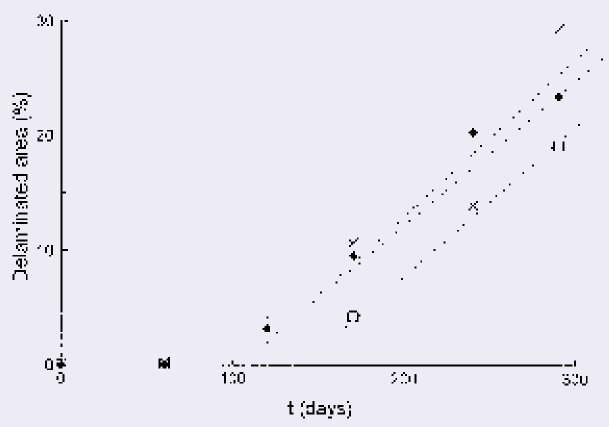

Figure 8—Area coverage from corrosion spots vs. exposure time at 3.5% NaCl.(□) Pure epoxy resin coatings, (x) epoxy resin coatings filled with 15% w/w iron powder, (♦) epoxy resin coatings filled with 30% w/w iron powder.

oxidation of the iron grains themselves introduces microcracks and active paths in the polymer matrix of the coating where this process is originated.[26] This is more evident in the case of the 30% loading where a smaller amount of electrolyte penetrates the coating as a result of the barrier protection mechanism and, subsequently, fewer blisters that evolve into corrosion spots are formed.

The surface area coverage from corrosion spots was calculated from the sum of the corrosion spot areas per sample divided by the total sample area (*Figure* 8). The surface area coverage increases with time for all types of coatings. For up to 120 days of immersion, all coatings exhibit almost the same value of coverage. After 180 days the iron-filled coatings differentiate from the pure epoxy resin coating. From this point and up to 300 days, the percentage increases linearly and at almost the same rate for all types of coatings.

EIS measurements performed on these specimens[26] confirm these conclusions. In *Figure* 9 the plot of the constant phase element (CPE) constant for the coating, Y_f, is presented. The impedance response of the CPE is given by the formula, $Z = \frac{(j\omega)^{-n}}{Y_o}$ where ω is the angular frequency, Y_o is the amplitude of the CPE and n is the CPE exponent.[26] This figure reveals the two-stage process observed earlier in the case of the iron-filled coatings, while the pure epoxy coating curve remains almost stable with a few fluctuations.

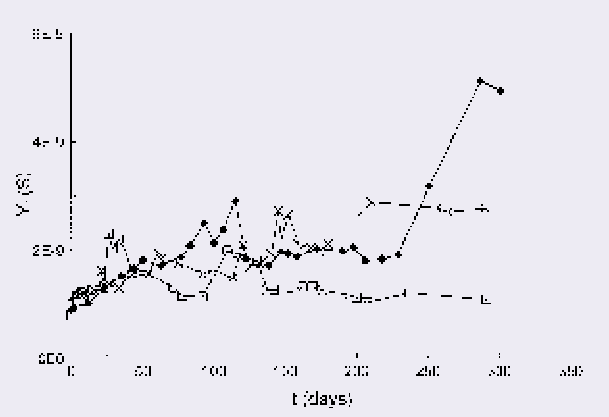

Figure 9—CPE constant Y_f vs. exposure time at 3.5% NaCl.(□) Pure epoxy resin coatings, (x) epoxy resin coatings filled with 15% w/w iron powder, (♦) epoxy resin coatings filled with 30% w/w iron powder.

CONCLUSIONS

The proposed system blends technologies from different areas (corrosion science, image processing, and database theory) in order to identify and classify corrosion generated defects. The procedures followed enable the automatic detection of a wide range of macroscopic and microscopic defects. Also, the database schema is designed in a way that image, defect, and electrochemical data are quickly and easily retrieved and complex queries can be answered.

Results obtained by the application of this system enabled the monitoring of the anticorrosive behavior of epoxy resin coatings filled with metal powders. In this case it was found that the iron powder-filled epoxy coatings produce fewer but larger corrosion spots compared to those of the pure epoxy coatings and that the inclusion of iron particles alters the impedance behavior of the coatings as a consequence of the creation of interfaces and corrosion products that increase the heterogeneity of the systems. However, the corrosion products fill the pathways blocking the intrusion of water. These conclusions were justified by the results of electrochemical impedance spectroscopy measurements.

References

(1) Murray, J.N. and Hack, H.P., *Corrosion (*NACE), 47, 480-489 (1991).
(2) Sobus, J., Pourdeyhimi, B., Xu., B., and Uleay, Y., *J. Text. Res*., 62, 26-39 (1992).
(3) Pourdeyhimi, B. and Nayernouri, A., “Evaluating Traffic Paint Degradation Using Image Analysis,” JOURNAL OF COATINGS TECHNOLOGY, *66*, No. 834, 51 (1994).
(4) McKnight, M.E. and Martin, J.W., “Detection and Quantitative Characterization of Blistering and Corrosion of Coatings on Steel Using Infrared Thermography,” JOURNAL OF COATINGS TECHNOLOGY, *71*, No. 775, 57 (1989).
(5) Fildes, J.M., Chen, P., and Zhan, X., Sensors Expo Conf., Boston, 1995.
(6) Schoff, C.K, “Surface Defects: Diagnosis and Cure,” JOURNAL OF COATINGS TECHNOLOGY, *71*, No. 888, 56 (1999).
(7) Bentz, D.P. and Martin, J.W., *J. Prot. Coat. Lin*., 4, 38-45 (1987).
(8) Martin, J.W. and McKnight, M.E., “Prediction of the Service Life of Coatings on Steel. Part III: Categorizing the Performance of Coating Systems on the Basis of Their Corrosion and Blister Patterns,” JOURNAL OF COATINGS TECHNOLOGY, *57*, No. 724, 49 (1985).
(9) Haralik, R.M., *Proc. of 4th Int. Joint Conf. Pattern Recog*., 45-60, 1979.
(10) Gonzalez, R.C. and Woods, R.E., *Digital Image Processing*, Addison-Wesley, New-York, 1992.
(11) Brzakovic, D., Paton, R., and Wang, R., *Computer Vision Graphics, Image Proc. Graphical Models and Iimage Proc.*, 53, 3, 258-268, 1991.

(12) Hansen, M. and Higgins, W., *Proc. IEEE Int. Conf. on Image Proc.*, 1994.
(13) Chen, D. and Wang, L., *Pattern Recogn.*, 24, 5 (1991).
(14) Tamura, H., Mori, S., and Yamawaki, T., *IEEE Trans. on Sys, Man, and Cyb*, SMC-8, 6, 1978.
(15) Stricker, M. and Orengo, M., *Proc. SPIE Storage and Retrieval for Image and Video Databases*, 1995.
(16) Russel, S. and Norvig, P. *Artifical Intelligence: A Modern Approach*, Prentice Hall, 1995.
(17) Sellis, T., Roussopoulos, N., and Faloutsos, C., *Proc. 13th VLDB Conf.*, 507-518, 1987.
(18) Faloutsos, C. and King-Ip Lin, *Proc. of Sigmoid*, 163-174, 1995.
(19) Codd, E.F., *Comm. ACM.*, 13, pp. 377-387 (1970).
(20) IS 9075, International Standard for Database Language, Document ISO/IEC9075, Melton, J. (Ed.), 1992.
(21) Rui, Y., Huang, T., and Chang, S.-F., *J. Visual Commun. Image Rep.*, 10, 1-23 (1999).
(22) Equitz, W. and Niblack, W., Technical Report RJ 9805 Computer Science, IBM Research Report, May 1994.
(23) Fagin R. and Wimmers, L., *Proc. of Intern. Conf. On Database Theory*, 1997.
(24) Faloutsos, C., Flickner, M., Niblack, W., Petkovic, D., Equitz, W., and Barber, R., Technical Report, IBM Research Report, 1993.
(25) Kouloumbi, N., Tsangaris, G.M., Kyvelidis, S.T., and Psarras, G.C., *Br. Corros. J.,* 34, 3 (1999).
(26) Kouloumbi, N., Tsangaris, G.M., and Kyvelidis, S.T., "Evalatuion of Corrosion Behavior of Metal-Filled Polymeric Coatings," JOURNAL OF COATINGS TECHNOLOGY, *66*, No. 839, 83 (1994).